Delay-Sensitive Coflow Routing for Time-Varying Topology in LEO Computing-Aware Networks

Shuang Yu[1], Shushi Gu[1,2], Zhikai Zhang[1], Qinyu Zhang[1,2], Zihe Gao[3], Yulin Shi[3] and Wei Xiang[4]
[1] Guangdong Provincial Key Laboratory of Aerospace Communication and Networking Technology,
Harbin Institute of Technology (Shenzhen), Shenzhen, China, 518055
[2] Peng Cheng Laboratory, Shenzhen, China, 518052
[3] China Academy of Space Technology, Beijing, China, 100094
[4] La Trobe University, Melbourne, VIC, Australia, 3086
{22S152062, 19B952013}@stu.hit.edu.cn; {gushushi, zqy}@hit.edu.cn;
biblejiayou@163.com; 429076118@qq.com; w.xiang@latrobe.edu.au

***Abstract*—Low earth orbit (LEO) computing-aware networks (LCANs) are proposed as an intelligent information infrastructure providing a solution for delay-sensitive computing tasks worldwide. The utilization of distributed computing architecture in an LCAN is emerging as a prospective resolution to cope with the limited computational resources of single satellite. Distributed computing depends on the exchange of information between worker nodes, as a type of concurrent and interrelated data flows called *coflow*. However, huge delay of coflow transmission is caused by the time-varying network topology and dynamic ISL conditions in an LCAN. To solve this problem, we establish an LCAN topology model, elaborating the orbit movement and ISL connectivity. Then we propose a novel time-varying graph to depict coflow transmission, which can improve the adaptability of coflow routing. Based on the proposed time-varying graph, we formulate coflow routing problem as a path combinatorial optimization and present an iterative heuristic algorithm named dynamic priority coflow routing (DPCoR). The DPCoR can dynamically adjust the priorities of coflow according to their increments to CCT, and thereby ensure that flows with high priorities for better routing paths. Furthermore, we compare DPCoR with traditional flow routing schemes, i.e., equal-cost multipath routing (ECMP) and software defined routing algorithm (SDRA) in various LCAN scenarios with different numbers of worker nodes, workloads and link conditions. The simulation results demonstrated that DPCoR algorithm can reduce the coflow completion time (CCT) effectively.**

***Index Terms*—LCAN, coflow routing, time-varying graph, DPCoR, CCT**

I. Introduction

Low earth orbit (LEO) computing-aware networks (LCAN) can facilitate the efficient utilization of on-board real-time communication and computing resources, schedule different applications to the appropriate satellite computing nodes [1]. To solve the problem that the computing resources on satellites are extremely limited, it is planned to deploy distributed computing architecture in the LCAN, to significantly enhance the overall efficiency of delay-sensitive computing tasks [2].

Distributed computing relies on the exchange of intermediate information between worker nodes, which is a kind of concurrent data flows, called *coflow*. The transmission of coflow occupies more than 50% of the job completion time, making it a key issue for task execution efficiency [3]. Continuous efforts have been devoted to solving coflow routing issues. [4] first identified bottleneck flows by assessing flow rate and transmitted bytes, then allocates bandwidth for other flows to match the bottleneck rate. Software-defined network (SDN) has been widely used in distributed computing network, because it can improve the flexibility of coflow management [5]. Moreover, the application of SDN for coflow routing and bandwidth allocation in a fat-tree network topology has been explored in [6]. However, the above coflow routing and scheduling algorithms focused on the terrestrial distributed networks scenarios. How to address the challenges posed by complex and dynamic topologies in LCAN, remains an imperative issue for effective coflow routing in satellite network, which motivates our work.

Many scholars use graph models to design routing algorithms in LEO satellite networks. Departing from static snapshot graphs, various time-varying graphs have been emerged, as well as corresponding routing strategies subsequently. The time-expanded graph (TEG) duplicates the original networks for each time slot, builds edges connecting each node, whose copy at the next slot is to represent data storage [7]. Based on TEG, the multicast time-expanded graph (MTEG) is further proposed to depict the across-time multicast transmission accurately in [8]. In [9], on the basis of weighted time-space evolution graph, a inter-satellite links (ISLs) utility-based dynamic routing algorithm is proposed to improve the adaptability of routing.

Unfortunately, the aforementioned dynamic routing algorithms applied in LEO networks fairly distribute link resources to flows in coflow set, emphasizing the improvement of average delay. Therefore, reducing average routing time does not necessarily indicate better overall transmission performance. Actually, in computing tasks, different flows contribute un-

This work is supported by the National Key Research and Development Program of China under Grant 2022YFB2902501, the National Natural Sciences Foundation of China under Grant 62271165 and Grant 62027802, the Guangdong Basic and Applied Basic Research Foundation under Grant 2023A1515030297, and the Shenzhen Science and Technology Program ZDSYS20210623091808025 and Stable Support Plan Program GXWD20231129102638002.

979-8-3503-8741-4/24/$31.00 ©2024 IEEE

equally to the coflow completion time (CCT), resulting in bad performance in traditional routing algorithms. In recent years, there has been some research on coflow routing in satellite distributed computing networks [10], but no consideration has been given to the possible links interruption caused by the dynamic topology. To bridge the gap, we attempt to propose a more suitable coflow routing algorithm for time-varying topology in LCAN, i.e., dynamic priority coflow routing (DPCoR). In summary, the main contributions of this paper can be summarized as follows:

1) We elaborate the connectivity of ISLs in LCAN topology. And a time-varying graph model is proposed to depict the dynamic transmission process of coflow. In this graph model, the feasible path set of the coflow set can be calculated. Then, the optimal coflow routing problem can be formulated into a path combinatorial optimization problem.

2) A heuristic algorithm DPCoR is designed to minimize CCT, which can dynamically adjust the priority of coflow according to their contributions on CCT. Compared to traditional routing algorithms, DPCoR prioritizes assigning better transmission paths to high-priority flows, thereby improving the overall performance of coflow transmission.

3) Simulation results demonstrate that under the conditions of dynamic topology and limited link capacities, our proposed DPCoR achieves an average improvement of 38.8%, 23.5% and 9.9%, compared to Dijkstra shortest path algorithm (DSP), equal-cost multi-path routing (ECMP) [11], and software defined routing algorithm (SDRA) [12], respectively.

The rest of this paper is organized as follows. Section II presents system models. Section III formulates the problem and proposes the DPCoR algorithm. In Section IV, we conduct experiments and analyze results. Finally, Section V concludes our work.

II. System Model

A. LCAN Model

Currently, large-scale satellite Walker constellation can be categorized into two types: Walker Polar Constellation and Walker Delta Constellation. We focus on Walker-Delta constellations in LCAN, formalized as $M/H/Q$, where M is the total number of satellites, H is the number of orbits, and Q is the phase factor. The phase offset between adjacent orbits is denoted by $\triangle\psi = 2\pi Q/M$. ISLs that connect satellites within orbit plane are denoted as intra-plane ISLs, while ISLs connecting satellites in different planes are denoted as inter-plane ISLs.

We assume that LCAN employs the classical MapReduce framework for distributed computing, which comprises three stages: "Map", "Shuffle", and "Reduce". When SDN controller deployed on satellite receives a computational request, it generates a computing cluster, and allocates mapper and reducer nodes for the computing task. Particularly, the shuffle stage generates a substantial amount of concurrent data flows in a short period.

In the condition of time-varying topology and limited transmission bandwidths in the satellite environment, the transmission of coflow becomes a bottleneck for the computing capabilities of LCAN. The coflow on LCAN can be expressed as

$$F = \{f_i\} = \{(S_i, D_i)\}, \tag{1}$$

where f_i represents one of the N flows in the coflow, S_i represents the source node of f_i, D_i represents the destination node of f_i. Here, we assume that the information of f_i can be captured through upper-layer applications or obtained using existing prediction technologies, thus supporting the subsequent work in this paper.

B. ISL Model

The geocentric coordinate system is established as Fig. 1. The geometric point **O** is the origin of coordinates. The x-axis is on the equatorial plane and points to the vernal equinox point. The z-axis is perpendicular to the equatorial plane. The y-axis is perpendicular to x-axis and z-axis, constituting a right-handed system. The satellite nodes in LEO satellite network can be denoted by $V = \{v_1, v_2, \ldots, v_m, \ldots, v_M\}$. Given the inclination of the satellite orbit α, right ascension of ascending node (RAAN) β, and initial phase angle ϕ of satellite v. Then, the coordinate $(x(t), y(t), z(t))$ of LEO satellite v at any time t can be calculated as

$$\begin{cases} x(t) = (R_{\mathrm{E}} + h_{\mathrm{S}}) \cos\left(\arcsin\left(\sin\alpha \sin\mu\right)\right) \cos\left(\gamma\right) \\ y\left(t\right) = (R_{\mathrm{E}} + h_{\mathrm{S}}) \cos\left(\arcsin\left(\sin\alpha \sin\mu\right)\right) \sin\left(\gamma\right) \\ z\left(t\right) = (R_{\mathrm{E}} + h_{\mathrm{S}}) \sin\alpha \sin\mu \end{cases}, \tag{2}$$

and

$$\gamma = \beta + \arctan\left(\cos\alpha \tan\alpha\right), \tag{3}$$

where $\mu = \omega_{\mathrm{s}} t + \phi$ denotes the phase of satellite at time t, ω_{s} is the angular velocity of the satellite, h_{S} is altitude of satellites, and R_{E} is the average earth radius. The distance between satellites can be calculated in above coordinate system as

$$\begin{aligned} &d_{mn}(t) = \mathrm{dist}(v_m, v_n) \\ &= \sqrt[2]{(x_m(t) - x_n(t))^2 + (y_m(t) - y_n(t))^2 + (z_m(t) - z_n(t))^2}. \end{aligned} \tag{4}$$

In Walker-type constellation, inter-plane ISLs are generally considered stable because the distance of intra-plane ISL in the same orbit is a constant, while the distance of inter-plane ISLs between any two satellites in adjacent orbit planes changes periodically. As a result, inter-plane ISLs are temporary links. We will measure the connectivity of inter-plane ISLs according to geometric visibility, antenna steering capability and inter-satellite link capacity.

If the d_{mn} between satellites is longer than their LoS distance, the ISLs will be sheltered by the Earth, so the maximum line-of-sight distance d_{max} can be calculated as:

$$d_{\max} = 2\sqrt{(R_{\mathrm{E}} + h_{\mathrm{S}})^2 - (R_{\mathrm{E}} + h_{\mathrm{T}})^2}, \tag{5}$$

where R_{E} is the average earth radius, h_{T} is height of thermosphere.

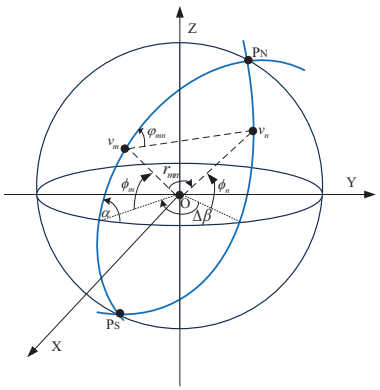

Fig. 1. Geometry of inter-plane ISL in geocentric coordinate.

As illustrated in Fig.1, two adjacent orbits intersect at points P_{N} and P_{S}. Given the difference of RAAN $\triangle\beta$ between two orbits, based on the spherical trigonometry, the included angle Φ between two orbit planes is computed by

$$\Phi = \arccos\left(\frac{\cos\left(\triangle\beta\right) - \cos(\phi_N)\cos(\phi_N^{'})}{\sin(\phi_N)\sin(\phi_N^{'})}\right), \tag{6}$$

where ϕ_N and $\phi_N^{'}$ are phase angles from the ascending points of two orbits to the point P_N, respectively. Given the phase angles of satellites ϕ_m and ϕ_n, The angle distance r_{mn} between satellites v_m and v_n is calculated by

$$\begin{aligned}\cos(r_{mn}) = \cos(\phi_m - \phi_N)\cos(\phi_n - \phi_N^{'}) + \\ \sin(\phi_m - \phi_N)\sin(\phi_n - \phi_N^{'})\cos(\Phi)\end{aligned}. \tag{7}$$

Then the azimuth angle φ_{mn} from satellites v_m to v_n in Fig.1 can be computed by

$$\cos(\varphi_{mn}) = \frac{\cos(\phi_m - \phi_N^{'}) - \cos(\phi_n + -\phi_N)\cos(r_{mn})}{\sin(\phi_m - \phi_N)\sin(r_{mn})}, \tag{8}$$

We can further calculate the second partial derivative of φ_{mn} versus r_{mn}. When φ_{mn} is minimized, the limit approaches to infinity as r_{mn} tends to zero.

$$\lim_{r_{mn}\to 0}\frac{\partial^2\cos(\varphi_{mn})}{\partial r_{mn}^2} = \infty. \tag{9}$$

The fast change of φ_{mn} along r_{mn} implies that when satellites approach the intersection points in polar zone, the change rate of φ_{mn} is maximized, which poses great difficult to the tracking and aiming of the satellite antenna. Here we assume that inter-plane links are closed to maintain communication quality when the angle distance of satellites is less than r_{min}, and the corresponding minimum distance of ISL is

$$d_{\min} = 2R\sin(\frac{r_{\min}}{2}). \tag{10}$$

Inter-satellite communication is mainly affected by free space path loss and the thermal noise is assumed to be additive white Gaussian noise (AWGN). Given the carrier frequency f and the velocity of light c, the transmission loss in free space can be obtained by

$$L_{mn} = (\frac{4\pi d_{mn} f}{c})^{-2}, \tag{11}$$

Assume that the transmission power P_t is fixed for all satellites and which are equipped with same directionaL antennas with perfect beam steering capabilities. Let P_{r}, G_{r} and G_{t} denote the transmitting power, the transmitting gain and the receiving gain, respectively. Then, the signal-to-noise ratio between v_m and v_n can be expressed as

$$SNR_{mn} = \frac{P_{mn}^{\mathrm{r}}}{N_0 B} = \frac{P_{\mathrm{t}}G_{\mathrm{t}}G_{\mathrm{t}}}{k_{\mathrm{B}}\tau B L_{mn}}, \tag{12}$$

where N_0 denotes additive AWGN and B is ISL bandwidth, k_{B} denotes the Boltzmann constant, and τ is the thermal noise in Kelvin. Additionally, P_{mn}^{r} is the received signal power. According to Shannon formula, we can calculate the ISL capacity C_{mn} as

$$C_{mn} = B\log_2\left(1 + \frac{P_{\mathrm{t}}G_{\mathrm{t}}G_{\mathrm{r}}}{k_{\mathrm{B}}\tau B L_{mn}}\right). \tag{13}$$

Supposing the minimum capacity of inter-satellite is C_{min}, if $C_{mn}(t) > C_{\min}$, the ISL between v_m and v_n is connected, otherwise the ISL is interrupted.

C. Coflow Transmission Time-Varying Graphs

A classic satellite network connection can be modeled as mesh topology: every satellite node usually has two intra-plane ISLs and two inter-plane ISLs. In this way, the topology of LCAN can be viewed as a Manhattan network. The 2D topology illustration is shown in Fig.2(a). By combining the time-varying topology and the definition of coflow set, we can construct a time-varying coflow transmission graph for describing the transmission of coflow.

As shown in Fig.2, the coflow transmission in time-varying graph can be formulated as

$$\mathbf{G_T} = \{V, E, W, F\}, \tag{14}$$

where $V = \{v_1, v_2, \ldots, v_m, \ldots, v_M\}$ is set of satellites nodes, and $S, D \in V$ represent mapper node set and reducer node set respectively.

$E = \{e_{mn}, m, n = 1, 2, \ldots, M\}$ is the edge set of graphs and e_{mn} denotes the ISLs of graphs. Actually, e_{mn} is a function of time t, i.e.,

$$e_{mn}(t) = \begin{cases} 1, & d_{\min} \le d_{mn}(t) \le d_{\max} \bigcap C_{mn} \ge C_0 \\ 0, & \text{otherwise} \end{cases}. \tag{15}$$

$W = \{w_{mn}, m, n = 1, 2, \ldots, M\}$ is the weight factor of e_{mn}, whose physical meaning is the available transmission rate at time t, i.e.,

$$w_{mn}(t) = \begin{cases} C_{mn}(t), & d_{\min} \le d_{mn}(t) \le d_{\max} \bigcap C_{mn} \ge C_0 \\ 0, & \text{otherwise} \end{cases}. \tag{16}$$

As above-mentioned, F is a set of flows on graph. Due to topological changes, the transmission of flow f_i may be

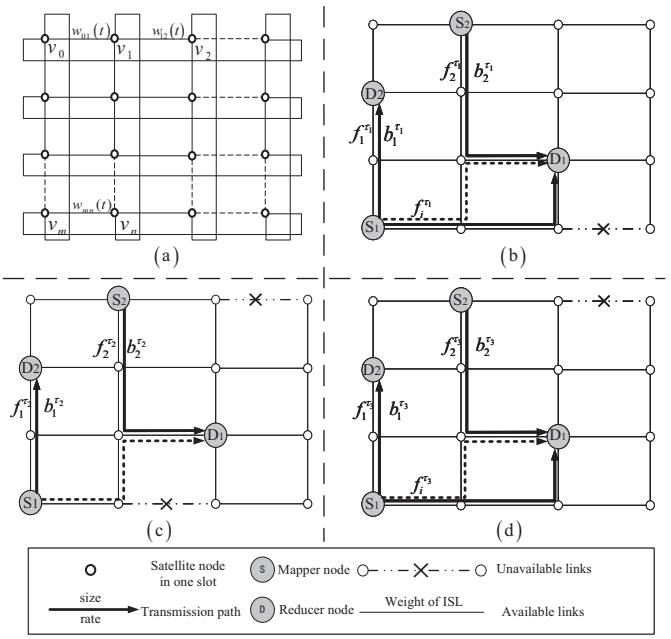

Fig. 2. Coflow transmission in time-varying graph. (a) time-varying graph model of LCAN, (b)(c)(d) coflow transmission over time slots τ_1, τ_2, τ_3, respectively.

interrupted, we can divide the transmission of f_i into several time slots $\{\tau_1, \tau_2, \ldots, \tau_q, \ldots, \tau_L\}$, and $f_i^{\tau_1}, f_i^{\tau_2}, \ldots, f_i^{\tau_L}$ are the transmitted flow sizes on different slots.

Fig.2 (b), (c) and (d) show the coflow transmission over three time slots $\{\tau_1, \tau_2, \tau_3\}$. The mapper nodes are S_1 and S_2, and reducer nodes are D_1 and D_2.

The satellite distributed computing cluster is a part of the satellite topology, as shown in Fig.2 (b), (c), and (d), the connectivity of the ISLs in three time slots is dynamic, which causes the diversity of flow transmit rate on different slots. For flow f_i, the rate on slots $\{\tau_1, \tau_2, \tau_3\}$ can be denoted as $b_i^{\tau_1}, b_i^{\tau_2}, b_i^{\tau_3}$. On slot τ_2, due to the disruption of ISL, the transmission of f_i is interrupted, and the wait time of f_i is defined as $\xi_{\text{wait}} = \tau_2$. Certainly, flow f_i has the choice to bypass the interrupted link by selecting the path as indicated by the dashed line in Fig.2 (b) (c) and (d). However, it will result in the competition for link transmission resources with flow f_2, potentially increasing CCT.

D. CCT model

For f_i in coflow set F, the flow transmission rate equals to the available transmission rate on the most congested link of whole path of f_i. After all the paths of f_i in coflow set F is confirmed, the transmission rate of flow f_i can be denoted as

$$b_i^*(t) = \{b_i^*(\tau_1), b_i^*(\tau_2), \ldots, b_i^*(\tau_q), \ldots, b_i^*(\tau_L)\}, \quad (17)$$

where $b_i^*(t)$ represents the transmission rate at slot t. Assuming the flow is transmitted over L time slots $\{\tau_1, \tau_2, \ldots, \tau_q, \ldots, \tau_L\}$, the flow f_i can be denoted as

$$f_i = f_i^{\tau_1} + f_i^{\tau_2} + \cdots f_i^{\tau_q} + \cdots f_i^{\tau_L}, \quad (18)$$

where $f_i^{\tau_q} = \tau_q * b_i^*(\tau_q)$ means that the size of the flow f_i on time slot τ_q is equal to the length of the time slot τ_q multiplied by the transmission rate allocated $b_i^*(\tau_q)$ during the time slot. Thus the transmission delay of flow f_i can be calculated as

$$\xi_{\text{transmit}} = \sum_{l=1}^{L-1} \tau_l + \frac{f_i^{\tau_L}}{b_i^*(t)}. \quad (19)$$

In summary, the completion time of coflow set in time-varying graph model will be composed of three parts: transmission delay, propagation delay, and waiting delay, which can be expressed as

$$T_i = \xi_{\text{transmit}} + \xi_{\text{wait}} + \xi_{\text{propaga}}. \quad (20)$$

The waiting delay of the transmission path results from link interruption and the propagation delay equals to distance of ISL divided by c. Moreover, CCT dependents on the slowest flow in transmission, obviously, we can obtain the final CCT as:

$$CCT = \max_{1 \le i \le N} T_i. \quad (21)$$

III. Proposed Coflow Routing Algorithm

A. Problem Formulation

Our goal is to minimize CCT, that is, to minimize the completion time of $f_i \in F$ that takes the longest time. Based on the previous analysis, CCT depends on the path selection of coflow. For each $f_i \in F$, there will be a path from the mapper to the reducer, which is expressed as

$$P = \{P_1, P_2, \ldots, P_i, \ldots P_N\}, \quad (22)$$

and

$$P_i = \left\{p_i^1, p_i^2, \ldots, p_i^k, \ldots, p_i^{M_i}\right\}, \quad (23)$$

where P_i represents the M_i feasible paths of f_i, p_i^k represents one of paths in P_i, and the optimal path of f_i is in P_i.

Here we use two binary variables $x_{mn}^{i,k}$ and $X_{p_i^k}$. $X_{p_i^k}$ indicates whether path p_i^k is selected. If p_i^k is selected by f_i, $X_{p_i^k} = 1$, otherwise $X_{p_i^k} = 0$. $x_{mn}^{i,k}$ determines whether p_i^k contains e_{mn}. If p_i^k contains e_{mn}, $x_{mn}^{i,k} = 1$, otherwise $x_{mn}^{i,k} = 0$.

After the transmission path of f_i is determined, the final path vector can be denoted as

$$P^* = \{p_1^*, p_2^*, \ldots, p_i^*, \ldots, p_N^*\}. \quad (24)$$

At the same time, the available capacity of the link is limited. For each time slot τ_i, and on all the ISL, i.e., e_{mn}, the following capacity constraint must be satisfied:

$$\sum_{i=1}^{N} x_{mn}^{i,*} b_i^*(t) \le C_{mn}(t) \ \forall v_m, v_n \in V, \forall t, \quad (25)$$

where $x_{mn}^{i,*}$ determines whether p_i^* contains e_{mn}, and $C_{mn}(t)$ is the capacity of link e_{mn} at time t. To guarantee the flow f_i

only use one path $p_i^k \in P_i$, it exists:

$$\sum_{p_i^k \epsilon P_i} X_{p_i^k} = 1, 1 \leq i \leq N. \tag{26}$$

In summary, the optimization problem of the minimum coflow transmission time in the time-varying topology can be expressed as follows:

$$min \quad CCT, \tag{27}$$

subject to:

(25), (26)

B. DPCoR algorithm

Standard algorithms will take a lot of time to get an optimal solution to the combinatorial optimization problem. When the number of working nodes and flows increase, it is not practical to solve the above optimization problems by traversing all path combinations.

In order to achieve lower complexity and efficient routing algorithm, we first assign priority attribute f_i^{pri} to f_i in the coflow set F. The flow priority is initialized by the transmission time of each flow taking in $\mathbf{G_T}$ without competition. Higher priorities are assigned to flows that take longer transmission time.

The fundamental principle guiding the selection from the available path set is to ensure that flow with higher priority find its optimal path, thereby minimizing conflicts with other flows with lower priority. Here, we introduce the concept of the max-conflict flow set Ω_{c}, which comprises the flows with the longest transmission time in the coflow set, i.e., the flows determining the CCT.

Therefore, throughout the iterative process of the algorithm, we consistently choose the flows with lower priority from Ω_{c} for path adjustments. Furthermore, it is essential to assess the suitability of different paths at the current iteration. A kind of suitability functions can be defined as

$$Score = \alpha_1\delta_1 + \alpha_2\delta_2 + (1 - \alpha_1 - \alpha_2)\delta_3, \tag{28}$$

where δ_1 denotes the increment of CCT caused by path change, δ_2 denotes the increment of other flows' transmission delay, and δ_3 denotes the increment in transmission time of the current path compared to the optimal path. We define α_1 and α_2 $(0 \leq \alpha_1 + \alpha_2 \leq 1, 0 \leq \alpha_1 \leq 1, 0 \leq \alpha_2 \leq 1)$ as weight factors, employed to measure the importance of different influencing factors during the path iteration process.

Algorithm 1 is built on the aforementioned idea to achieve the optimal solution through a step-by-step iterative approach. In Algorithm 1, after establishment of coflow transmission time-varying graph $\mathbf{G_T}$, line 3 calculates the set of reachable paths is obtained based on $\mathbf{G_T}$. Lines 4 to 8 involve initializing the priority ordering of flows based on the shortest transmission time of paths in the graph model. Lines 9 to 21 constitute the main iteration process of the algorithm. In each iteration, the algorithm identifies Ω_c, alters the path of the flow f_i with the lowest priority f_i^{pri} in the set, and computes the current path fitness score using (28). In line 20, the priority of the flow f_i that has just experienced a path change is set to the highest to prevent cyclic scheduling. Line 21 records optimal CCT and path set during the iteration process.

Algorithm 1: Dynamic Priority Coflow Routing (DP-CoR)

Input: $\mathbf{G_T} = \{V, E, W, F\}$
Output: P^*, CCT

1: Initialize LCAN computing cluster and current operating time
2: **for** $f_i \in F$ **do**
3: Calculate the reachable paths set P_i in $\mathbf{G_T}$
4: **for** $p_i \in P_i$ **do**
5: Calculate conflict-free transmission delay
6: **end for**
7: Calculate the shortest path of f_i and corresponding delay in $\mathbf{G_T}$
8: Initialize the priority f_i^{pri} according to the shortest path of f_i
9: **end for**
10: **while** $\Omega_{\text{c}} \neq \emptyset$ **do**
11: Select f_i with minimum f_i^{pri} in Ω_{c}
12: **for** $p_i \in P_i$ **do**
13: Calculate time increment of CCT: δ_1
14: Calculate time increment of other paths: δ_2
15: Calculate time increment of conflict-free path: δ_3
16: Calculate the fitness according to (28)
17: **end for**
18: Select p^* with best fitness
19: Assign $p^* \rightarrow p_i$
20: Increase the priority f_i^{pri} of f_i just changed path
21: Record the optimal P^*, CCT
22: **end while**
23: **return** P^*, CCT

IV. Simulation Results

In the simulation, we consider a Walker-delta constellation with arrangement (72/9/1). The specific simulation parameters are detailed in the Table I.

To verify the adaptability of the routing algorithm to the dynamic changes of topology, we intend to compare it with DSP, ECMP and SDRA. The ECMP is usually seen as the standardized routing scheme of modern data centers. SDRA obtains the routing path by centralized routing strategy. Furthermore, it can collect congestion status of the satellites in real time and bypass the congested ISLs to balance load.

As shown in Fig.3(a), fixing the total workloads, with increasing the number of worker nodes (decreasing the size of each flow), will cause the CCT decreasing. When we fix the number of worker nodes in Fig.3(b), the sizes of per flow increase as the workloads increases, so the CCT will also increases. Compared to the DSP, ECMP, and SDRA, the DPCoR reduces the CCT by nearly as 38.1%, 29.9%, and 10.1%, respectively. For the DSP, although it assigns the optimal path for each flow in the coflow set, it does not

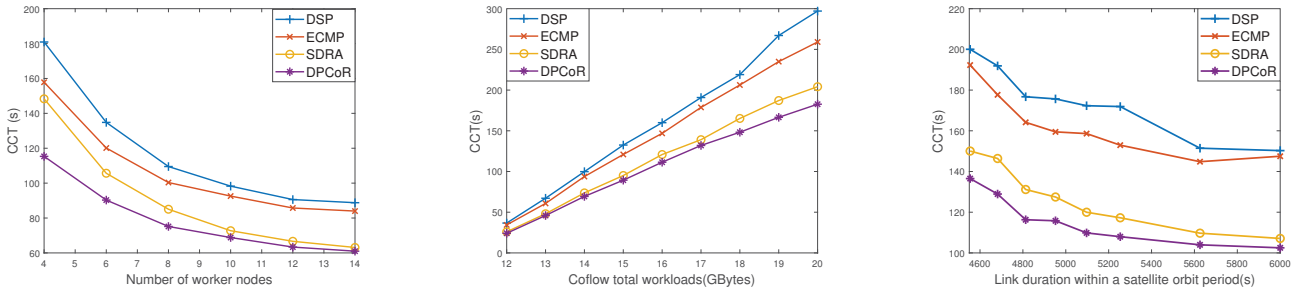

(a) CCT versus number of worker nodes. (b) CCT versus total workloads. (c) CCT versus link durations.

Fig. 3. CCTs of DPCoR compared with three traditional routing algorithms in different scenarios.

TABLE I
SIMULATION PARAMETERS

Symbol	Values	Symbol	Values
M	72	f	25 GHz
h_{S}	1150 Km	G_{t}	38.5 dB
H	9	G_{r}	38.5 dB
Q	1	P_t	50 W
α	53°	B	400 MHz
$\triangle\beta$	45°	τ	354.81 K

consider competition during flow transmission, resulting in link congestion. Therefore, the CCT of the DSP algorithm is the longest. Compared to the ECMP, DPCoR demonstrates superior performance. This is attributed to the fact that ECMP does not account for interruptions in the networks, resulting in poor load balancing performance. Although SDRA considers dynamic link performance and load balancing on network, however, it places emphasis on the average delay of routing without making a distinctive allocation of communication resources for flows within the coflow that contribute differently to CCT. Hence it fails to guarantee that flows that critical to computation delay occupy better ISLs, resulting in higher CCT than DPCoR.

Fig.3(c) illustrates that after changing the conditions for establishing ISLs, the available link establishment duration within one orbit period also changes. It is evident that all routing algorithms will increase in CCT as the available links resource decreasing. As the link interrupted time increasing, the CCT of DPCoR only rises by 15.0%, while ECMP experiences a 40% increase in CCT. In the scenario where satellite links are disconnected for up to 28.8% of the time in a period, DPCoR still achieves performance improvements of 27.3% and 9.1% compared to ECMP and SDRA, respectively.

V. Conclusion

In this paper, we attempt to use a novel time-varying topology model to depict dynamic coflow transmission in LCAN. We analyze the LCAN topology and establish the connectivity of ISLs model, and then we propose the concept of coflow transmission time-varying graph. Based on the information provided by graphs, we formulates the coflow routing problems into a path combinatorial optimization, and propose a heuristic routing algorithm DPCoR to ensure that flows with high priorities within coflow are minimally impacted by links interruptions and congestion. Simulation results demonstrate that DPCoR improves the adaptability to the dynamic topology of the LCAN, significantly reducing the CCT of the computing task.

References

[1] C. Peng, Y. He, S. Zhao, L. Song and B. Deng, "Integration of data center into the distributed satellite cluster networks: challenges, techniques, and trends," *IEEE Netw.*, vol. 37, no. 3, pp. 52-58, May 2023.

[2] S. Wang and Q. Li, "Satellite computing: vision and challenges," *IEEE Internet Things J.*, vol. 10, no. 24, pp. 22514-22529, Dec.15, 2023.

[3] S. Luo, P. Fan, H. Xing and H. Yu, "Meeting coflow deadlines in data center networks with policy-based selective completion," *IEEE/ACM Trans. Netw.*, vol. 30, no. 1, pp. 178-191, Oct. 2023.

[4] L. Liu *et al*., "Bottleneck-aware non-clairvoyant coflow scheduling with Fai," *IEEE Trans. Cloud Comput.*, vol. 11, no. 1, pp. 1011-1025, Jan. 2023.

[5] P. Qin, B. Dai, B. Huang, and G. Xu, "Bandwidth-aware scheduling with SDN in Hadoop: A new trend for big data," *IEEE Syst. J.*, vol. 11, no. 4, pp. 2337-2344, Dec. 2017.

[6] H. Tan *et al*., "Joint online coflow routing and scheduling in data center networks," *IEEE Trans. Netw.*, vol. 27, no. 5, pp. 1771-1786, Oct. 2019.

[7] C. Wang, Z. Ren, W. Cheng, S. Zheng, and H. Zhang, "Time-expanded graph-based dispersed computing policy for LEO space satellite computing," in *Proc. IEEE Wireless Commun. Netw. Conf. (WCNC)*, Nanjing, China, Mar. 2021, pp. 1-6.

[8] K. Shi, X. Zhang, S. Zhang, and H. Li, "Time-expanded graph based energy-efficient delay-bounded multicast over satellite networks," *IEEE Internet Things J.*, vol. 69, no. 9, pp. 10380-10384, Sep. 2020.

[9] Z. Han, C. Xu, G. Zhao, S. Wang, K. Cheng and S. Yu, "Time-varying topology model for dynamic routing in LEO satellite constellation networks," *IEEE Trans. Veh. Technol.*, vol. 72, no. 3, pp. 3440-3454, Mar. 2023.

[10] Z. Zhang, S. Gu, S. Li, Y. Yang, and Q. Zhang, "Multi-hop coflow routing for LEO distributed computation satellite networks," in *Proc. 96th. IEEE Veh. Technol. Conf. (VTC2022-Fall)*, London, United Kingdom, Sep. 2022, pp. 1-5.

[11] J. Liu, J. Huang, W. Li, J. Wang and T. He, "Asymmetry-aware load balancing with adaptive switching granularity in data center," *IEEE/ACM Trans. Netw.*, vol. 31, no. 3, pp. 1145-1158, Jun. 2023.

[12] Y. Zhu, L. Qian, L. Ding, F. Yang, C. Zhi, and T. Song, "Software defined routing algorithm in LEO satellite networks," in *Proc. Int. Conf. Electr. Eng. (ICELTICs)*, Banda Aceh, Indonesia, Oct. 2017, pp. 257-262.